Electronic Structure of $La_{2-x}Sr_xCuO_4$ in the Vicinity of the Superconductor-Insulator Transition

A. Ino[1*], C. Kim[2], M. Nakamura[3], T. Yoshida[1], T. Mizokawa[1], Z.-X. Shen[2], A. Fujimori[1], T. Kakeshita[4], H. Eisaki[4] and S. Uchida[4]

[1] *Department of Physics, University of Tokyo, Bunkyo-ku, Tokyo 113-0033, Japan*

[2] *Department of Applied Physics and Stanford Synchrotron Radiation Laboratory, Stanford University, Stanford, CA94305, USA*

[3] *Department of Physics, Nara University of Education, Takabatake-cho, Nara 630-8528, Japan*

[4] *Department of Superconductivity, University of Tokyo, Bunkyo-ku, Tokyo 113-8656, Japan*

(February 1, 2008)

We report on the result of angle-resolved photoemission (ARPES) study of $La_{2-x}Sr_xCuO_4$ (LSCO) from an optimally doped superconductor ($x = 0.15$) to an antiferromagnetic insulator ($x = 0$). Near the superconductor-insulator transition (SIT) $x \sim 0.05$, spectral weight is transferred with hole doping between two coexisting components, suggesting a microscopic inhomogeneity of the doped-hole distribution. For the underdoped LSCO ($x \leq 0.12$), the dispersive band crossing the Fermi level becomes invisible in the $(0,0)$–(π,π) direction unlike $Bi_2Sr_2CaCu_2O_{8+y}$. These observations may be reconciled with the evolution of holes in the insulator into fluctuating stripes in the superconductor.

PACS numbers: 74.25.Jb, 71.30.+h, 74.72.Dn, 79.60.-i, 74.62.Dh

The key issue to clarify the nature of high-temperature superconductivity in the cuprates is how the electronic structure evolves from the antiferromagnetic insulator (AFI) to the superconductor (SC) with hole doping. For the hole-doped CuO_2 planes in the superconductors, band dispersions and Fermi surfaces have been extensively studied by angle-resolved photoemission spectroscopy (ARPES) primarily on $Bi_2Sr_2CaCu_2O_{8+y}$ (BSCCO)[1–4]. Also for the undoped AFI, band dispersions have been observed for $Sr_2CuO_2Cl_2$[5,6]. However, the band structures of the AFI and the SC are distinctly different and ARPES data have been lacking around the boundary between the AFI and the SC. In order to reveal the missing link, the present ARPES study has been performed on $La_{2-x}Sr_xCuO_4$ (LSCO), which covers continuously from the SC to the AFI in a single system.

In addition, the family of LSCO systems show a suppression of T_c at a hole concentration $\delta \simeq 1/8$, while the BSCCO system does not. As the origin of the anomaly at $\delta \simeq 1/8$, the instability towards the spin-charge order in a stripe form has been extensively discussed on the basis of the incommensurate peaks in inelastic neutron scattering (INS)[7–9]. Comparing the ARPES spectra of LSCO and BSCCO will help us to clarify the impact of the stripe fluctuations.

In the present paper, we discuss the novel observation of two spectral components coexisting around the SIT ($x \sim 0.05$), the unusual disappearance of the Fermi surface near $(\pi/2, \pi/2)$ in the underdoped LSCO ($x \leq 0.12$)[4], and their relevance to the stripe fluctuations.

The ARPES measurements were carried out at beamline 5-3 of Stanford Synchrotron Radiation Laboratory (SSRL). Incident photons had an energy of 29 eV and were linearly polarized. The total energy resolution was approximately 45 meV and the angular resolution was ±1 degree. Single crystals of LSCO were grown by the traveling-solvent floating-zone method and then annealed so that the oxygen content became stoichiometric. The accuracy of the hole concentration δ was ±0.01. The $x = 0$ samples were slightly hole doped by excess oxygen so that $\delta \simeq 0.005$ was deduced from its Néel temperature $T_N = 220$ K[10]. The spectrometer was kept in an ultra high vacuum better than 5×10^{-11} Torr during the measurements. The samples were cleaved *in situ* by hitting a post glued on the top of the samples. The measurements were done only at low temperatures ($T \sim 11$ K), because the surfaces degraded rapidly at higher temperatures. Throughout the paper, the spectral intensity for different angles are normalized to the intensity of the incident light. In the analysis, the spectrum at (0,0) is assumed to represent the angle-independent background, because emission from the states of $d_{x^2-y^2}$ symmetry is not allowed for the direction normal to the CuO_2 plane due to a selection rule. Indeed, Figs. 1 and 3 show that spectra in the vicinity of the Fermi level (E_F) are angle-independent, when there are no dispersive features.

ARPES spectra along $(0,0) \rightarrow (\pi,0) \rightarrow (\pi,\pi)$ clearly shows angle dependence as shown in Fig. 1. Even though spectral features are broad for underdoped and heavily undoped cuprates[1,2,5,6], the dispersive component emerging around $\vec{k} = (\pi, 0)$ is sufficiently strong compared to the angle-independent background. Figure 2 shows the doping dependence of the ARPES spectrum at $(\pi, 0)$. As reported previously[4], a relatively sharp peak is present just below E_F for the optimally doped sample ($x = 0.15$). For the underdoped samples ($x = 0.12, 0.10$ and 0.07), the peak is broadened and shifted downwards. When the hole concentration is further decreased to the vicinity of the SIT ($x = 0.05$), the peak near E_F rapidly loses its intensity and concomitantly another broad feature appears around -0.55 eV. In the AFI phase ($x = 0$), the peak near E_F disappears entirely while the structure around

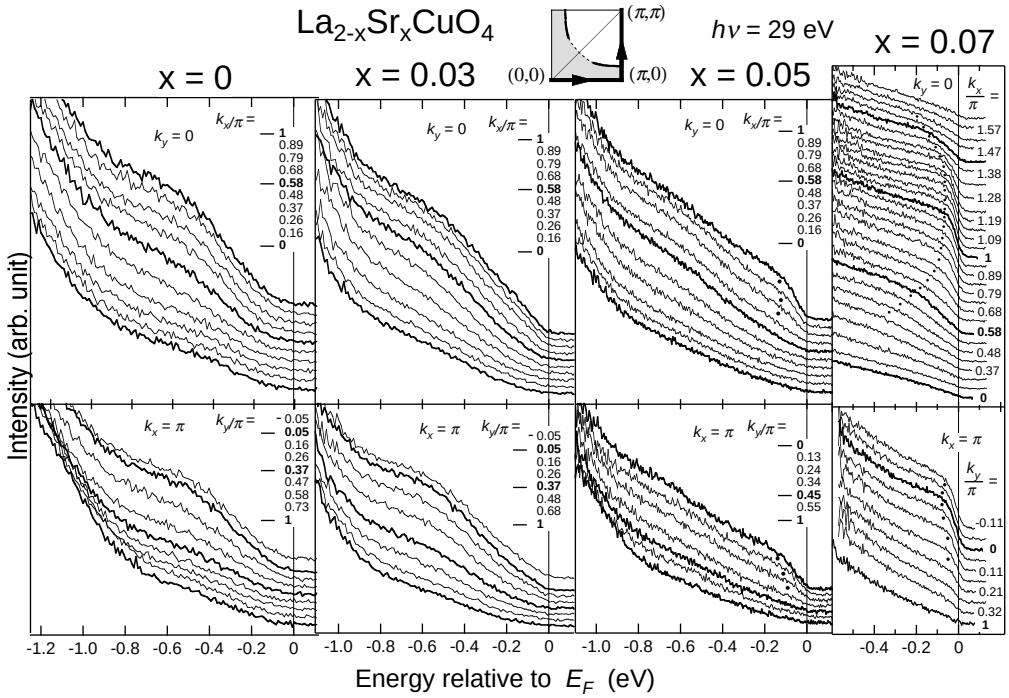

FIG. 1. ARPES spectra of $La_{2-x}Sr_xCuO_4$ (LSCO) for $x = 0$, 0.03, 0.05 and 0.07, taken along $(0,0) \rightarrow (\pi,0)$ (upper panels) and $(\pi,0) \rightarrow (\pi,\pi)$ (lower panels). The dispersive component emerging around $\vec{k} = (\pi,0)$ is sufficiently strong compared to the angle-independent background. Inset shows the Brillouin zone and the Fermi surface of underdoped LSCO[4].

~ -0.55 eV becomes predominant. As for LSCO, Fig. 2 is different from the scenario that a single peak is shifted downwards and continuously evolves from the SC into the AFI as seen in BSCCO and $Ca_2CuO_2Cl_2$[11], and rather indicates that the spectral weight is transferred between the two features originated from the SC and the AFI, and

On the other hand, ARPES spectra in the (0,0)-(π,π) direction show a different doping dependence. The spectra for representative doping levels are shown in Fig. 3. For the optimally doped sample ($x = 0.15$), one can identify a band crossing E_F around (0.4π,0.4π), although the dispersive feature is considerably weak. For the underdoped samples ($x = 0.12, 0.10$ and 0.07), the band crossing E_F disappears, even though the system is still superconducting. The invisible band crossing along (0,0)-(π,π) is reproduced for several samples for $0.07 \leq x \leq 0.12$, excluding accidentally inferior surfaces as its origin. For the insulating sample ($x = 0.03$ and 0), a broad feature appears around ~ -0.45 eV near (π/2,π/2), correlated with the growth of the broad structure around ~ -0.55 eV at (π,0).

Overall dispersions of the spectral features have been derived from the ARPES spectra by taking second derivatives as shown in Fig. 4. The band near E_F for $x = 0.05$, 0.07, 0.10 and 0.12 has a dispersion similar to that for $x = 0.15$ around $(\pi,0)$: when one goes as $(0,0) \rightarrow (\pi,0) \rightarrow (\pi,\pi)$, the band approaches E_F until $\sim$(0.8π,0), stays there until (π,0), then further approaches E_F and goes above E_F through the superconducting gap around $\sim(\pi,\pi/4)$. The band seen near E_F should be responsible for the superconductivity. On the other hand, the dispersions of the broad feature seen around -0.5 eV are almost the same among $x = 0$, 0.03 and 0.05 and similar to the band dispersion of the undoped CuO_2 plane in $Sr_2CuO_2Cl_2$[5,6] and $PrBa_2Cu_3O_7$[12]. Along the $(0,0) \rightarrow (\pi,\pi)$ cut, the broad peak moves upwards, reaches a band maximum (~ -0.45 eV) around $(\pi/2,\pi/2)$ and then disappears. The broad peak emerges in going from $(0,0)$ to $(\pi,0)$ and then disappears between $(0,0)$ and (π,π). Therefore, the band around -0.5 eV originates from the lower Hubbard band (LHB) of the AFI.

In Fig. 5(a), the dispersive components of the ARPES spectra are compared between (π,0) and $\sim$(π/2,π/2). Around the SIT ($x \sim 0.05$), the two spectral features coexist at (π,0), while only one broad peak is observed at $\sim$(π/2,π/2). This excludes extrinsic origins for the two structures such as a partial charge-up of the sample. Figure 5(b) demonstrates that the spectral lineshape at (π,0) and the relative intensity of two structures are quite systematically evolves with hole doping, indicating that surfaces of good quality were consistently obtained for all the doping levels. The spectral weight transfer is reminiscent of earlier discussion based on angle-integrated data of LSCO and $Nd_{2-x}Ce_xCuO_4$[13]. A possible origin for the coexistence of the two spectral features is a phase separation into hole-poor antiferromagnetic (AF) domains and hole-rich superconducting domains. The spectra around SIT may be regarded as a superposition of the spectra of the SC and the AFI, as illustrated in Fig. 6 (b). Indeed,

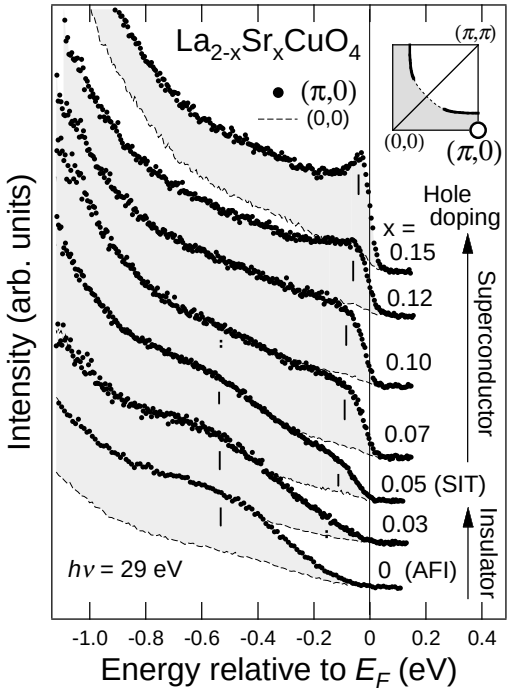

FIG. 2. Doping dependence of ARPES spectra at $\vec{k} = (\pi, 0)$. The spectra have been normalized to the intensity of the valence-band peak at ~ -3 eV. Each thin dashed line denotes the spectrum at (0,0) representing the angle-independent background. The spectrum of $x = 0.05$ at the superconductor-insulator transition (SIT) point shows two spectral features associated with the antiferromagnetic insulator (AFI) and the superconductor (SC) at ~ -0.5 eV and ~ -0.1 eV, respectively.

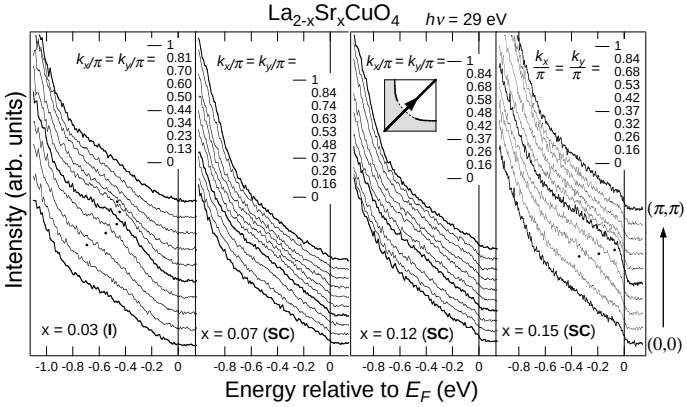

FIG. 3. Doping dependence of ARPES spectra taken along (0,0)→(π,π). While a broad feature dispersing across E_F is identified for $x = 0.15$, the dispersive band is absent near E_F for $x = 0.12$ and 0.07, even though the system is superconducting. For $x = 0.03$, a band appears at ~ -0.45 eV around $(\pi/2,\pi/2)$.

when holes are doped into La_2CuO_{4+y} with excess oxygens, such a phase separation occurs macroscopically as revealed by, e.g., neutron diffraction[14], but corresponding observation has never been reported for the Sr-doped

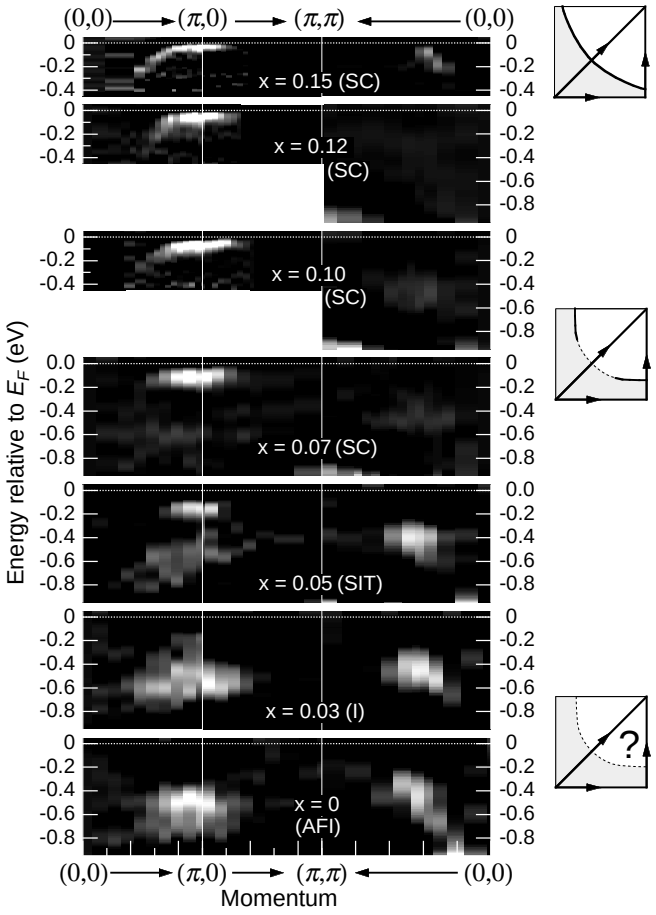

FIG. 4. Band structure deduced from the ARPES spectra by taking the second derivatives after subtracting the angle-independent background. For $x = 0.05$, while the band around -0.1 eV originates from the band in the underdoped superconductor ($x = 0.12$, 0.10 and 0.07), the band around -0.5 eV appears to originate from the lower Hubbard band in the antiferromagnetic insulator ($x = 0$).

LSCO system. A more likely interpretation is a microscopic inhomogeneity of the hole density in the sense that the doped holes are segregated in boundaries of AF domains on the scale of several atomic distances. Indeed, μ^+SR[15] and ^{139}La NQR[16] experiments have shown the presence of a local magnetic field in the so-called spin-glass phase [Fig. 6 (a)]. Then, since the present spectra were taken above the spin-glass transition temperature, splitting into the two structures would be due to dynamical fluctuations of such a microscopic phase separation. Furthermore, the microscopic phase separation may explain why the chemical potential is pinned against hole doping for $x \lesssim 0.12$[17]. However, as for the underdoped BSCCO, the splitting of the two components by ~ 0.5 eV has not been reported so far and the peak at $(\pi,0)$ seems to be shifted smoothly in going from the SC to the AFI[11]. The difference might imply that the tendency toward the hole segregation is stronger in LSCO than in BSCCO.

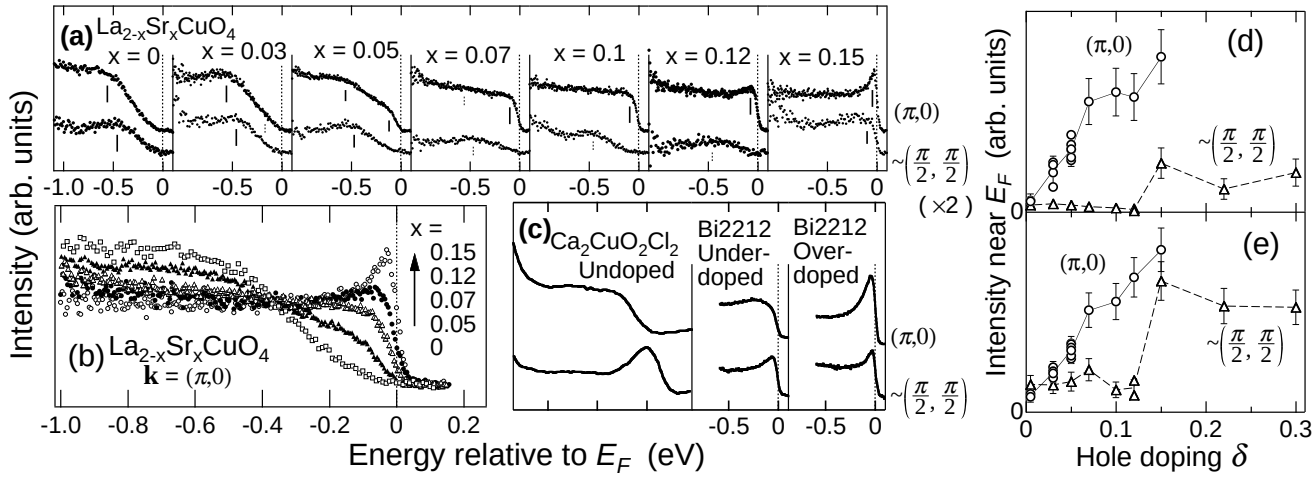

FIG. 5. (a) Comparison between the spectra at $(\pi,0)$ and $\sim(\pi/2,\pi/2)$ (multiplied by 2) for $La_{2-x}Sr_xCuO_4$. The spectrum at (0,0) has been subtracted as the angle-independent background. (b) Spectra at $(\pi,0)$, normalized to the integrated intensity in $E > -0.9$ eV, clearly demonstrating the systematic evolution with hole doping. (c) ARPES spectra for other cuprates: Ca_2CuOCl_2 (undoped) and $Bi_2Sr_2CaCu_2O_{8+y}$ (underdoped and overdoped), shown in a similar way to (a), taken from Ref. 6 and 11, respectively. While the lineshapes at $(\pi,0)$ are similar between $La_{2-x}Sr_xCuO_4$ and $Bi_2Sr_2CaCu_2O_{8+y}$, the lineshapes at $\sim(\pi/2,\pi/2)$ are quite different. (d)(e) Doping dependence of the spectral intensity near E_F ($E > -0.2$ eV) at $(\pi,0)$ (◯) and at $\sim(\pi/2,\pi/2)$ (△), normalized to the intensity of the valence-band peak of the $(\pi,0)$ spectra at ~ -3 eV and to the integrated intensity in $E > -0.9$ eV for (d) and (e), respectively.

The ARPES spectra of LSCO are compared with those of BSCCO[6,18] in Figs. 5 (a) and (c). Whereas the lineshapes at $(\pi,0)$ are similar between LSCO and BSCCO irrespective of doping levels, the spectra near $(\pi/2,\pi/2)$ are quite different: while the peak near E_F is sharp for both the overdoped and underdoped BSCCO, one finds no well-defined feature around E_F for underdoped LSCO. This difference is likely to be related with the stripe fluctuations, which have more static tendency in LSCO than in BSCCO, judging from the suppression of T_c at $\delta \simeq 1/8$. Also for the BSCCO system, it has been reported that the sharp peak near E_F is suppressed near $(\pi/2, \pi/2)$ upon Zn-doping, which is considered to pin the dynamical stripe correlations[19,20]. The absence of the band crossing E_F near $(\pi/2, \pi/2)$ may be reconciled with the vertically and horizontally oriented stripes in LSCO[7]. Intuitively, while the system may be metallic along the half-filled stripes, namely, in the $(0, 0)$-$(\pi, 0)$ or $(0, 0)$-$(0, \pi)$ direction, the low-energy excitations should be strongly suppressed in the directions crossing all the stripes such as the $(0, 0)$-(π, π) direction. This conjecture was supported by a recent numerical study of small clusters with charge stripes[21], and is consistent with the suppression of the Hall coefficient in the stripe-ordered state of $La_{1.6-x}Nd_{0.4}Sr_xCuO_4$ for $x < 1/8$[22].

The doping dependence of the spectral intensity near E_F ($E > -0.2$ eV) is shown in Figs. 5 (d) and (e) for two normalization methods. Note that the essential features are independent of normalization. Our picture of the evolution of the spectral weight is schematically drawn in Fig. 6. In the ARPES spectra, the intensity near E_F appears at $(\pi,0)$ with hole doping for $x \gtrsim 0.05$, where the incommensurability of the spin fluctuations also arises according to the INS study[23]. On the other hand, the intensity near $(\pi/2,\pi/2)$ remains suppressed with hole doping for the entire underdoped region ($0.05 \lesssim x \lesssim 0.12$). Hence, one may think that the segregated holes for $x \sim 0.05$ already start to be arranged vertically and horizontally. Therefore we propose that the hole-rich boundaries of the AF domains around the SIT continuously evolves into the stripe correlations in the underdoped SC. In going from $x = 0.12$ to 0.15, the Fermi-surface crossing appears in the (0,0)-(π,π) direction, probably corresponding to the phenomenon that the incommensurability in INS saturates for $x \gtrsim 0.15$[23]. This may be understood that the doped holes in excess of $x = 1/8$ overflow the saturated stripes and that the two-dimensional electronic structure recovers.

In conclusion, we have shown that the SC and AFI characters coexist in the ARPES spectra in the vicinity of the SIT for LSCO. The band crossing E_F disappears near $(\pi/2,\pi/2)$ for the underdoped LSCO, associated with the formation of the dynamical stripes. The present observations provide a new perspective of how the holes doped in the AFI evolve into the fluctuating stripes in the underdoped SC. Mechanism in which the SC to AFI transition occurs is a subject of strong theoretical interest[24,25] and should be addressed by further studies.

We would like to thank T. Tohyama and S. Maekawa for enlightening discussions. This work was supported by the New Energy and Industrial Technology Development Organization (NEDO), Special Coordination Fund for Promoting Science and Technology from the Science and Technology Agency of Japan, the U. S. DOE, Office

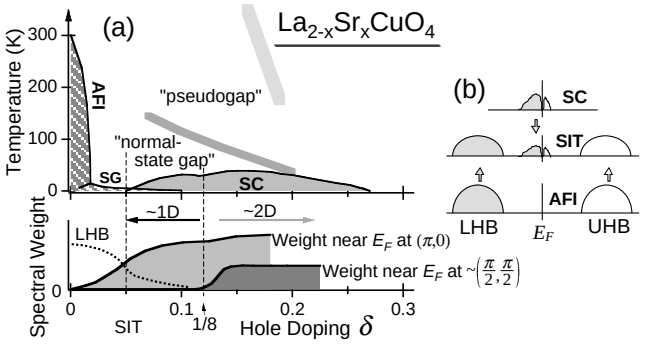

FIG. 6. (a) Schematic picture of the evolution of spectral weight with hole doping for the lower Hubbard band (LHB) and the band near E_F at $(\pi, 0)$ and at $\sim (\pi/2, \pi/2)$. The phase diagram was drawn after Refs. 15 and 26 (SG: so-called spin-glass phase). (b) Schematic drawing indicating that the spectra around the SIT ($x \sim 0.05$) consist of two kinds of electronic states derived from the SC and the AFI.

of Basic Energy Science and Division of Material Science. Stanford Synchrotron Radiation Laboratory is operated by the U. S. DOE, Office of Basic Energy Sciences, Division of Chemical Sciences.

---

* Present address: Japan Atomic Research Institute (JAERI), SPring-8, Hyogo 679-5148, Japan.

[1] Z.-X. Shen, W. E. Spicer, D. M. King, D. S. Dessau and B. O. Wells, Science **267**, 343 (1995).

[2] D. S. Marshall, D. S. Dessau, A. G. Loeser, C.-H. Park, A. Y. Matsuura, J. N. Eckstein, I. Bozovic, P. Fournier, A. Kapitulnik, W. E. Spicer and Z.-X. Shen, Phys. Rev. Lett. **76**, 4841 (1996).

[3] H. Ding, A. F. Bellman, J. C. Campuzano, M. Randeria, M. R. Norman, T. Yokoya, T. Taakahashi, H. Katayama-Yoshida, T. Mochiku, K. Kadowaki, G. Jennings and G. P. Brivio, Phys. Rev. Lett. **76**, 1533 (1996).

[4] A. Ino, C. Kim, T. Mizokawa, Z.-X. Shen, A. Fujimori, M. Takaba, K. Tamasaku, H. Eisaki and S. Uchida, J. Phys. Soc. Jpn., **68**, 1496 (1999).

[5] B. O. Wells, Z.-X. Shen, A. Matsuura, D. M. King, M. A. Kastner, M. Greven and R. J. Birgeneau, Phys. Rev. Lett. **74**, 964 (1995).

[6] C. Kim, P. J. White, Z.-X. Shen, T. Tohyama, Y. Shibata, S. Maekawa, B. O. Wells, Y. J. Kim, B. J. Birgeneau, and M. A. Kastner, Phys. Rev. Lett. **80**, 4245 (1998).

[7] J. M. Tranquada, B. J. Sternlieb, J. D. Axe, Y Nakamura, and S. Uchida, Nature **375**, 561 (1995).

[8] A. Bianconi, N. L. Saini, A. Lanzara, M. Missori, T. Rossetti, H. Oyanagi, H. Yamaguchi, K. Oka and T. Ito, Phys. Rev. Lett. **76**, 3412 (1996).

[9] J. Zaanen and A. M. Oleś, Ann. Physik **5**, 224 (1996).

[10] C. Y. Chen, R. J. Birgeneau, M. A. Kastner, N. W. Preyer and T. Thio, Phys. Rev. B **43**, 392 (1991).

[11] F. Ronning, C. Kim, D. L. Feng, D. S. Marshall, A. G. Loeser, L. L. Miller, J. N. Eckstein, I. Bozovic and Z.-X. Shen, Science **282**, 2067 (1998).

[12] T. Mizokawa, C. Kim, Z.-X. Shen, A. Ino, A. Fujimori, M. Goto, H. Eisaki, S. Uchida, M. Tagami, K. Yoshida, A. I. Rykov, Y. Siobara and S. Tajima, Phys. Rev. B **60**, 12335 (1999).

[13] J. W. Allen, C. G. Olson, M. B. Maple, J.-S. Kang, L. Z. Liu, J.-H. Park, R. O. Anderson, W. P. Ellis, J. T. Markert, Y. Dalichaouch and R. Liu, Phys. Rev. Lett. **64**, 595 (1990).

[14] P. G. Radaelli, J. D. Jorgensen, R. Kleb, B. A. Hunter, F. C. Chou and D. C. Johnston, Phys. Rev. B **49**, 6239 (1994).

[15] Ch. Niedermayer, C. Bernhard, T. Blasius, A. Golnik, A. Moodenbaugh and J. I. Budnick, Phys. Rev. Lett. **80**, 3843 (1998).

[16] J. H. Cho, F. Borsa, D. C. Johnston and D. R. Torgeson, Phys. Rev. B **46**, 3179 (1992).

[17] A. Ino, T. Mizokawa, A. Fujimori, K. Tamasaku, H. Eisaki, S. Uchida, T. Kimura, T. Sasagawa and K. Kishio, Phys. Rev. Lett. **79**, 2101 (1997).

[18] Z.-X. Shen and J. R. Schrieffer, Phys. Rev. Lett. **78**, 1771 (1997).

[19] P. J. White, Z.-X. Shen, D. L. Feng, C. Kim, M.-Z. Hasan, J. M. Harris, A. G. Loeser, H. Ikeda, R. Yoshizaki, G. D. Gu and N. Koshizuka, cond-mat/9901349.

[20] M. Akoshima, T. Noji, Y. Ono and T. Koike, Phys. Rev. B **57**, 7491 (1998).

[21] T. Tohyama, S. Nagai, Y. Shibata and S. Maekawa, Phys. Rev. Lett. **82**, 4910 (1999).

[22] T. Noda, H. Eisaki and S. Uchida, Science **286**, 265 (1999).

[23] K. Yamada, C. H. Lee, K. Kurahashi, J. Wada, S. Wakimoto, S. Ueki, H. Kimura, Y. Endoh, S. Hosoya, G. Shirane, R. J. Birgeneau, M. Greven, M. A. Kastner and Y. J. Kim, Phys. Rev. B **57**, 6165 (1998).

[24] S.-C. Zhang, Science **275**, 1089 (1997).

[25] F. F. Assaad, M. Imada and D. J. Scalapino, Phys. Rev. Lett. **77**, 4592 (1996).

[26] N. Momono, M. Ido, T. Nakano, M. Oda, Y. Okajima and K. Yamaya, Physica C **233**, 395 (1994).